NANO LETTERS

pubs.acs.org/NanoLett Letter

A Resonance-Sensitive Ultralow-Frequency Raman Mode in Twisted Bilayer Graphene

Shuowen Yan, Jianqi Huang, He Hao, Ge Song, Yuechen Wang, Hailin Peng, Teng Yang, Jin Zhang, and Lianming Tong*

Cite This: *Nano Lett.* 2024, 24, 7879−7885 Read Online

ACCESS | Metrics & More | Article Recommendations | Supporting Information

Downloaded via PEKING UNIV on September 11, 2024 at 06:37:47 (UTC).
See https://pubs.acs.org/sharingguidelines for options on how to legitimately share published articles.

ABSTRACT: Twisted bilayer graphene (tBLG) possesses intriguing physical properties including unconventional superconductivity, enhanced light−matter interaction due to the formation of van Hove singularities (vHS), and a divergence of density of states in the electronic band structures. The vHS energy band gap provides optical resonant transition channels that can be tuned by the twist angle and interlayer coupling. Raman spectroscopy provides rich information on the vHS structure of tBLG. Here, we report the discovery of an ultralow-frequency Raman mode at ~49 cm^{-1} in tBLG. This mode is assigned to the combination of ZA (an out-of-plane acoustic phonon) and TA (a transverse acoustic phonon) phonons, and the Raman scattering is proposed to occur at the so-called mini-valley. This mode is found to be particularly sensitive to the change in vHS in tBLG. Our findings may deepen the understanding of Raman scattering in tBLG and help to reveal vHS-related electron−phonon interactions in tBLG.

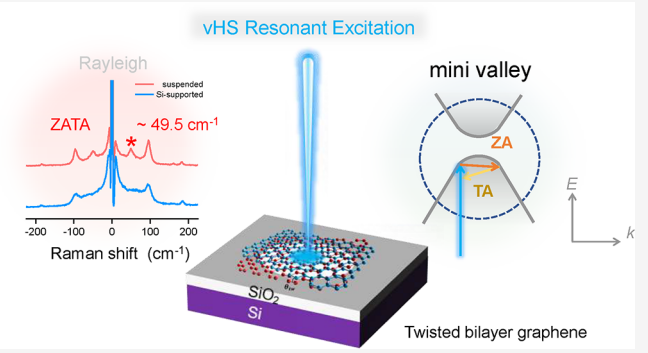

KEYWORDS: *twisted bilayer graphene (tBLG), van Hove singularity (vHS), resonance Raman scattering, anti-Stokes Raman scattering*

Twist stacking provides an effective way to alter interlayer coupling and electronic properties of 2D materials.[1] Twisted bilayer graphene (tBLG) has been attracting wide attention of scientists since it exhibits unconventional superconductivities for magic-angle graphene species,[2,3] Moiré superlattice,[4] excitons,[5−7] chiral optical response,[8] and so on. Besides, anticrossed linear band structure generates van Hove singularities (vHS),[9,10] which supports tunable optical resonant transition from the UV to mid-IR depending on the twist angle, thus making tBLG a potential candidate for on-chip optoelectronic devices.[11] Therefore, developing fast and comprehensive characterization of the crystal and energy band structure of tBLG is of great significance.

Raman scattering provides a convenient and noninvasive spectroscopic tool to reveal the crystal structure of tBLG through characteristic vibrational modes,[9,12] such as G mode with a specific Raman shift ~1580 cm^{-1} representing C−C bond stretching, the layer breathing (LB) mode with ~96 cm^{-1} in tBLG[13−15] reflecting interlayer breathing vibration, as well as R or R′ mode[16,17] and a series of phonon modes activated by the Moiré superlattice.[18] In fact, mini-valley structure is formed in tBLG and has been reported to support rich but complicated Raman scattering by means of vHS resonance and unique valley band structure.[19] However, due to difficulty on theory prediction of tBLG phonon dispersion,[20] a full understanding about Raman scattering of tBLG is still lacking. Hence, the experimental exploration of new phonon modes for tBLG is important, particularly for further revealing the electron−phonon interaction due to interlayer coupling and vHS resonance.

Herein, we report an ultralow-frequency Raman mode at ~49 cm^{-1} of tBLG under vHS resonance excitation. Through polarized dependence of Raman intensity and the analysis of phonon dispersion of AB-stacked bilayer graphene, we tentatively assign this mode to the combination of ZA and TA phonons, therefore named as ZATA in this work, and find out that it shows a narrower resonant profile than G and LB modes. Our findings suggest that this Raman mode can be used to detect the subtle change of vHS band structure and contribute to deepening the understanding of electron−phonon interaction at the vHS resonance of tBLG.

tBLG with arbitrary twist angle were grown using the chemical vapor deposition (CVD) method.[21] The CVD-grown tBLG samples were then transferred onto patterned SiO_2/Si substrate with holes of 3−5 μm in diameter by the wet

Received: February 28, 2024
Revised: June 15, 2024
Accepted: June 17, 2024
Published: June 20, 2024

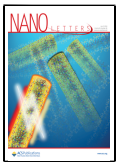

ACS Publications © 2024 American Chemical Society

https://doi.org/10.1021/acs.nanolett.4c01018
Nano Lett. 2024, 24, 7879−7885

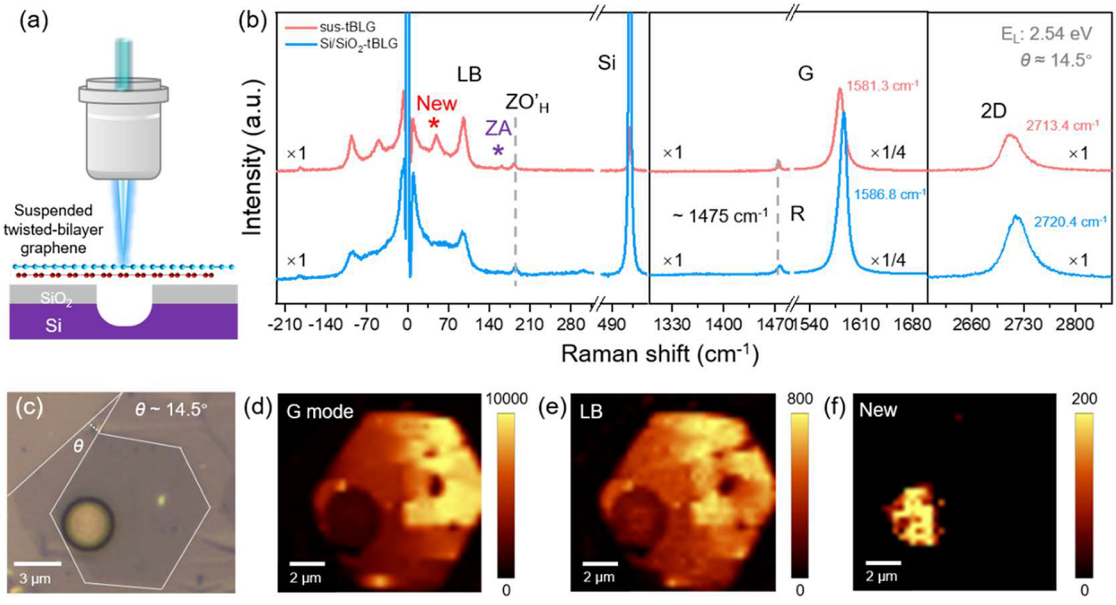

Figure 1. (a) Schematic of the Raman measurement on suspended tBLG. (b) Raman spectra of Si/SiO_2-supported and suspended ~14.5° tBLG excited by a 2.54 eV laser. (c) Optical microscopy (OM) image of the 14.5° tBLG. The white lines depict the edges of the bottom and top layers of tBLG, and θ denotes the twist angle. (d–f) Raman intensity mapping of the G mode, the layer breathing (LB) mode, and the new mode, respectively.

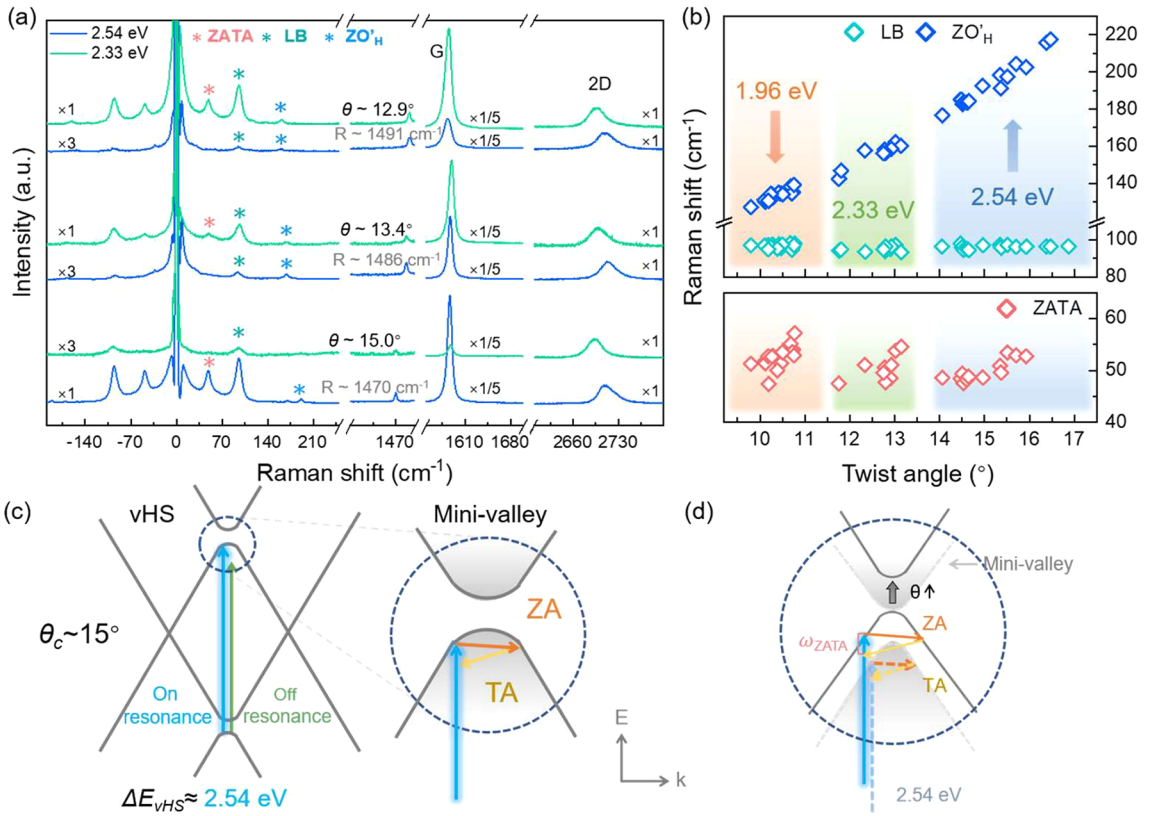

Figure 2. (a) Representative spectra of 3 tBLGs with twist angles 12.9°, 13.4°, and 15° excited by 2.54 and 2.33 eV. The red, green, and blue stars denote the positions of the ZATA, LB, and ZO'_H modes. (b) Raman frequencies of ZO'_H, LB, and ZATA as a function of twist angle. (c) Illustration of band structure of tBLG 15°, excited both by 2.33 and 2.54 eV, corresponding to weak or strong resonance. (d) Illustration of scattering pathway of ZATA mode with small (light gray curve) and large (dark gray curve) twist angles. For increased twist angle θ, the frequency of the ZATA mode increases, as indicated by variation from dashed pink and yellow lines to solid ones.

chemical method (see Supporting Information I for details), as schematically shown in Figure 1a. The optical microscopy (OM) image of a suspended tBLG is shown in Figure 1c. The twist angle θ is estimated to be 14.5° from the edges of the bottom and top graphene layers depicted by the white lines, which is also confirmed by the peak position of the R mode

https://doi.org/10.1021/acs.nanolett.4c01018
Nano Lett. 2024, 24, 7879−7885

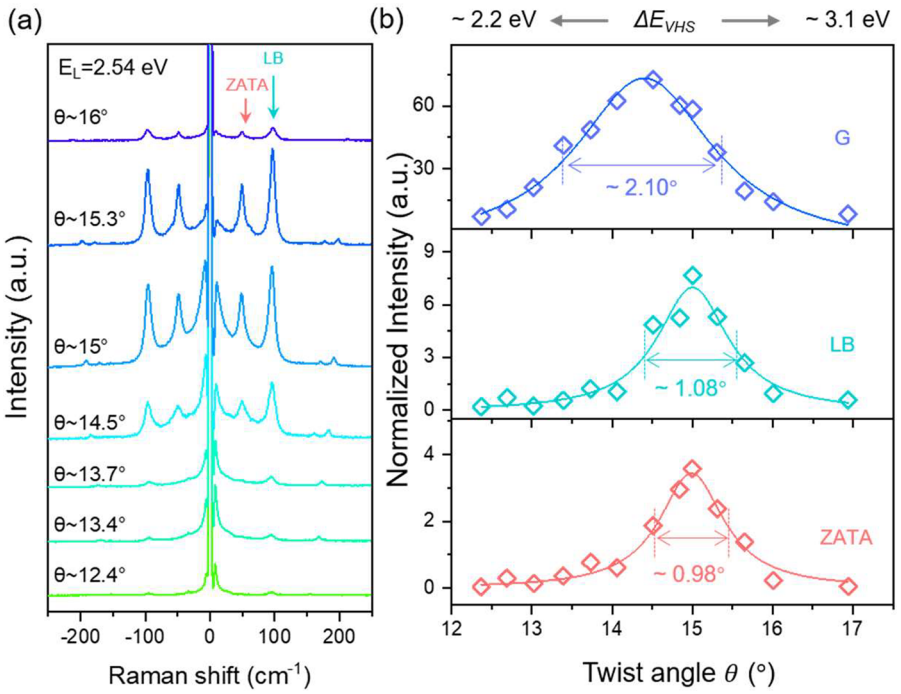

Figure 3. (a) Raman spectra of 7 tBLG samples with a twist angle ranging from 12° to 16° excited by 2.54 eV. (b) Resonance profile of intensity of G mode and LB and ZATA mode normalized by the Si Raman mode (~520.7 cm^{-1}) as a function of twist angles.

shown in Figure 1b. The corresponding atomic force microscopy (AFM) image is shown in Figure S1. The Raman spectra of both suspended and supported tBLG with $\theta \sim 14.5°$ excited by 2.54 eV are shown in Figure 1b. The G mode of suspended tBLG (1581.3 cm^{-1}) exhibits a red-shift of 5.5 cm^{-1} compared to that on the SiO_2/Si substrate (1586.8 cm^{-1}), while the 2D band in suspended area (2713.4 cm^{-1}) also exhibits a red-shift of about 7.0 cm^{-1} compared with that on SiO_2/Si substrate (2720.4 cm^{-1}). These spectral differences could be attributed to the lack of doping and suspension-induced tensile strain. In general, charge doping on graphene would cause a blue-shift of the G mode,[22] while tensile biaxial strain would cause a G mode red-shift without splitting.[23] The correlation between ω_G and ω_{2D} of suspended and Si/SiO_2 supported tBLG, together with the height profile measured by atomic force microscopy (AFM), is plotted in Figure S1 of the Supporting Information.[24] The R mode appears at 1475 cm^{-1} in both spectra, indicating that the twist angle is 14.5°,[17] consistent with optical image observation. In the low-frequency region, the layer-breathing (LB) mode and the ZO'_H mode show the same Raman shift at 95.5 and 185.8 cm^{-1} for the suspended and supported regions. Interestingly, a new peak at 49 cm^{-1} appears for the suspended tBLG with the suppression of a low-frequency signal. According to previous studies,[13,25,26] this low-frequency signal could be assigned to electronic Raman scattering (ERS) resulting from free carriers in doped Si, which might overwhelm the signal of the new Raman modes.[26]

The Raman intensity maps of the G, LB, and the new mode are shown in Figure 1d–f, respectively. Because of the lack of optical interference in the SiO_2 layer,[27] the intensities of the G mode and 2D mode are lower in the suspended region than that supported on the substrate. However, the Raman mode at 49 cm^{-1} apparently only shows up in the suspended region.

In order to analyze the symmetry of this phonon mode, we performed polarized Raman measurement, as shown in Figure S2. The polarization-angle-dependent Raman spectra and the polar plots of both the LB and the new mode are shown in Supporting Information III and Figure S3. It is seen that the new mode shows a similar angle dependence with the LB mode, that is, maximum intensity for $\beta = 0°$ (polarization of polarizer I is parallel to that of polarizer II) and minimum intensity for $\beta = 90°$ (polarization of polarizer I is perpendicular to that of polarizer II). This result indicates that the new mode can be reasonably assigned to A symmetry and is an out-of-plane mode. It should be noted that there is only one LB mode, and the shear mode does not exist in tBLG.[14,15] Due to the difficulty in the theoretical calculation of phonon dispersion curve of tBLG, we take the phonon dispersion of bilayer graphene in Figure S4 as reference, where the ZA, LO′, TO′, LA, and TA modes can be found in the low-frequency region below 50 cm^{-1}. From the symmetry analysis and the calculation of the probability of combinational modes that show up at 49 cm^{-1}, we tentatively assign this mode to the combinational mode of TA and ZA phonons and name it as ZATA in this work (see Supporting Information IV for details).

The dispersion of the ZATA mode is explored by measuring suspended tBLG of twist angles from ~9° to ~16° using 1.96, 2.33, and 2.54 eV. We should note that the change of vHS band gap by tuning the twist angle for a fixed laser line is in principle analogous to the scan of energy of laser lines. In Figure 2a, we show the Raman spectra of tBLG samples with twist angles 12.9°, 13.4°, and 15° for 2.54 and 2.33 eV excitation. It is seen that for ~12.9° and ~13.4° tBLG, the Raman scattering is more resonantly enhanced under 2.33 eV excitation than 2.54 eV, while for ~15° tBLG, the resonance enhancement is stronger under 2.54 eV excitation. The ZATA mode shows resonance dependence similar to that of the G and LB modes and only appears under the most resonant excitation.

https://doi.org/10.1021/acs.nanolett.4c01018
Nano Lett. 2024, 24, 7879−7885

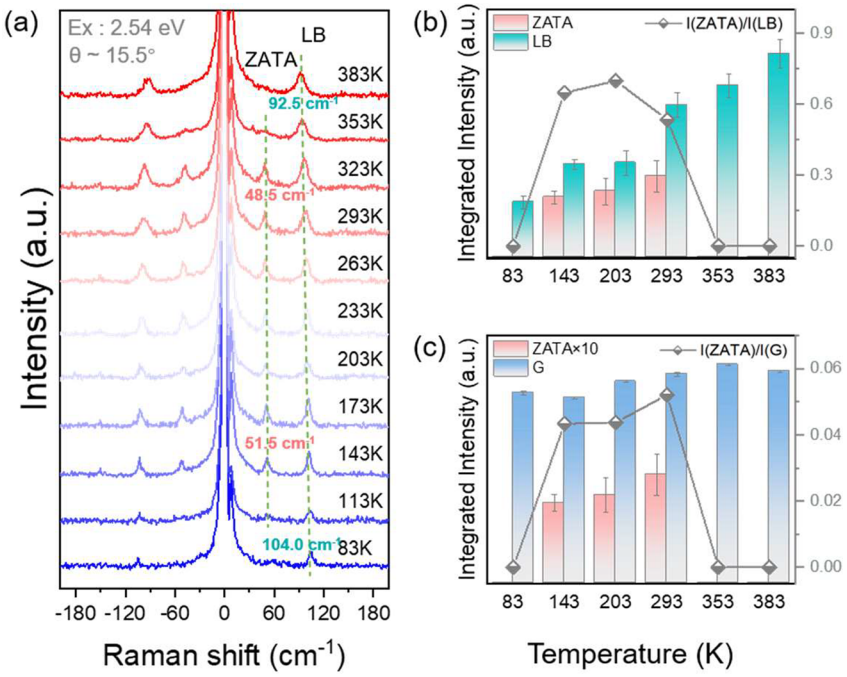

Figure 4. (a) *In situ* temperature-dependent Raman spectra of suspended tBLG (15.5°) from 83 to 383 K, excited by 2.54 eV. (b, c) Integrated intensities of ZATA, LB modes (b) and ZATA, G modes (c) and the corresponding intensity ratio is depicted by half-filled diamond.

Further, in order to find out whether ZATA is a first-order or second-order Raman mode, several tBLG samples with different angles were measured with 3 laser lines, and the twist angle dependence of ZATA frequency was observed, strongly implying that it is a double-resonance Raman mode. Figure 2b shows the Raman frequencies of the ZO'_H, LB, and ZATA modes as a function of twist angle. With increasing twist angle from 9.8° to 16.9°, the Raman shift of the ZO'_H mode increases from 127.2 to 217.7 cm^{-1}, and the LB mode remains unchanged at ~96.1 cm^{-1}, which is in accordance with the literature.[13,16] However, the Raman shift of ZATA mode ω_{ZATA} depends on both the excitation energy and twist angle. ω_{ZATA} increases slightly from 47.4 to 57.1 cm^{-1} with increasing twist angle from 9.8° to 10.8° when excited by 1.96 eV, from 47.5 to 54.6 cm^{-1} with twist angle from 11.7° to 13.2° for 2.33 eV, and from 48.6 to 52.7 cm^{-1} with twist angle from 14.0° to 15.9° for 2.54 eV. As the appearance of the ZATA mode requires strong vHS resonance, for a fixed twist angle, we could observe the ZATA mode for only one of the three excitation energies. Nevertheless, this twist angle dependence of ω_{ZATA} for fixed laser energy confirms that it is a double-resonance scattering process. The scattering pathway is proposed in Figure 2c, where the scattering of the ZA and TA phonons with tiny momentum at the mini-valley[19] is depicted. For a fixed laser energy, the increase of twist angle, and thus the vHS band gap, leads to the optical transition from a momentum shifted further away from the Γ-point of the phonon Brillouin zone and accordingly higher energy of ZA and TA phonons. The line width of the ZATA mode is comparable to those of the LB and G modes and decreases slightly with increasing twist angle, which might be related to complicated double-resonance Raman scattering in tBLG.[28]

The resonance dependence of the ZATA mode is analyzed by extracting the peak intensity with twist angles from 12° to 16° excited by 2.54 eV. Typical Raman spectra are shown in Figure 3a, and the normalized intensities of the G, LB, and ZATA modes as a function of twist angles are plotted in Figure 3b. It is noted that the critical angle for the resonance enhancement of the ZATA mode at 15.0° is larger than that of the G band at 14.4°. This suggests that the optical transition energy where the ZATA mode is activated is different from the vHS band gap, where the resonance for the G band occurs. Interestingly, the resonance window for the ZATA mode is 0.98°, which is much narrower than that for the G band, 2.10°, indicating that the ZATA mode is more sensitive to the change of resonance conditions.

The temperature-dependent Raman spectra of a 15.5° tBLG excited by the 2.54 eV laser are measured and are shown in Figure 4a. Generally, the intensity of resonant Raman scattering could be tuned by temperature, mainly due to modulation of temperature on the energy band that thus influences the probability of resonant Raman scattering.[29,30] In accordance with refs 30−32, the change of temperature modulates the energy band structure, and the decrease of band gap was reported for Si, two-dimensional semiconductors with increasing temperature.

In Figure 4b,c, the intensity of the G and LB modes, depicted by the histogram, increases with temperature rising from 83 to 383 K. Different from the LB mode, the intensity of the G mode slightly increases with temperature rising, which could be probably due to wide resonance window of G mode in accordance with Figure 3b. Instead, the ZATA mode appears at temperatures higher than 113 K, and the intensity increases to the maximum at 293 K, then decreases at higher temperature, and disappears at 353 K, exhibiting a much higher sensitivity to temperature, as depicted by the intensity ratio of ZATA/LB in Figure 4b as well as ZATA/G in Figure 4c, which both increase first from 83 to 203 K and then begin to decline from 293 K and down to 0 at 383 K. Cycling temperature-dependent Raman spectra in Figure S6 suggests that appearance and disappearance of ZATA are not due to thermal degradation. Comparing with the monotonic increase

https://doi.org/10.1021/acs.nanolett.4c01018
Nano Lett. 2024, 24, 7879−7885

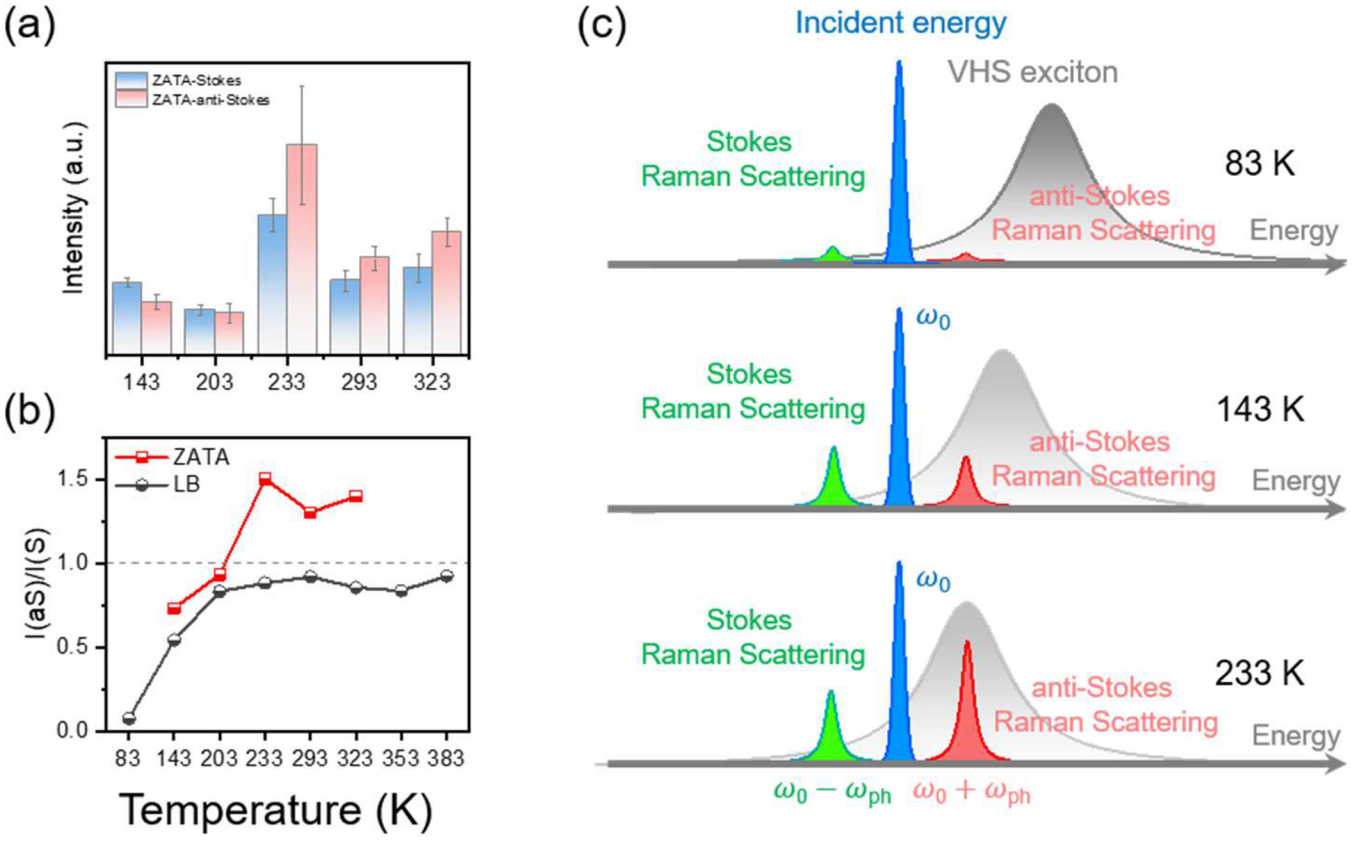

Figure 5. (a) Stokes and anti-Stokes scattering intensity of ZATA mode with increasing temperature. (b) Intensity ratio of Stokes and anti-Stokes scattering of ZATA and LB with increasing temperature. (c) Possible mechanism of vHS exciton-assisted ZATA anti-Stokes enhancement. Reproduced with permission from ref 30.

of G and LB intensities, it is plausible to conclude that the ZATA mode is more sensitive to the change of vHS resonance than the G and LB modes. Besides, we also observe that the Raman shift of LB red-shifts from ∼104.0 cm^{-1} at 83 K to ∼92.5 cm^{-1} at 383 K monotonically. However, it is hard to distinguish whether temperature-induced phonon softening, change of electron energy band, or both above contribute to the red-shift of ZATA Raman frequency from ∼51.5 cm^{-1} at 143 K to ∼48.5 cm^{-1} at 323 K monotonically. Comparing with the monotonic increase of G and LB intensities, it is plausible to conclude that the ZATA mode is more sensitive to the change of vHS resonance than the G and LB modes.

Further, we find out that the ZATA mode shows anomalously high anti-Stokes/Stokes intensity ratio I_{aS}/I_S, as illustrated in Figure 5a. The I_{aS}/I_S values of the LB mode are shown in Figure 5b for comparison. For the LB mode, the I_{aS}/I_S values increases with increasing temperature, which follows the Bose−Einstein distribution of phonons given by

$$\frac{I_{aS}}{I_S} = \frac{{\omega_{aS}}^4}{{\omega_S}^4} \exp\left[\frac{-\hbar\omega_{ph}}{k_B T}\right]$$

where ω_{aS} and ω_S are frequencies of scattered light, $\hbar$ is the reduced Planck constant, k_B is the Boltzmann constant, and ω_{ph} is the frequency of phonons. The I_{aS}/I_S value of the ZATA mode is significantly larger than that of the LB mode and even exceeds 1 at temperatures higher than 233 K. Besides, twist-angle-dependent Raman Stokes and anti-Stokes intensity, I_{aS}/I_S, in tBLG are shown in Figure S5, where ZATA anti-Stokes Raman scattering shows higher intensity than Stokes scattering when $\theta \sim 15°$ and $\theta \sim 15.3°$. Such an anomalous I_{aS}/I_S value can be explained by the exciton resonance and strong electron−phonon coupling and might be related to red-detuned excitation of resonance, as reported in refs 30, 33, and 34 and schematically shown in Figure 5c.

In conclusion, this work studied an ultralow-frequency Raman mode at ∼49 cm^{-1} in suspended tBLG and systematically investigated its resonance dependence. We discussed the symmetry of the new mode through polarized Raman and assigned it to the combination of ZA and TA phonons, which is scattered at the bottom of the mini-valley around vHS. Temperature-dependent and twist-angle-dependent Raman spectra suggested that ZATA shows a narrower resonant profile than LB and G modes. Besides, ZATA showed higher anti-Stokes intensity than Stokes intensity in tBLG with twist angle ranging from 15° to 15.3° or at the range from 143 to 323 K for 15.5° tBLG under 2.54 eV resonance excitation. We also performed power-dependent Raman measurement of suspended tBLG as shown in Figure S7, which shows a linear power dependence under laser powers up to 1.0 mW. Although theoretical simulation is necessary to further understand the physical origin of this mode, the findings in this work suggest that this mode is more sensitive to the vHS resonance than the G and LB modes and could be used to reveal subtle changes of environment of suspended tBLG and may offer inspirations and enlightenments of resonant Raman scattering on characterizing energy band structure of other twist-stacked 2D materials.

https://doi.org/10.1021/acs.nanolett.4c01018
Nano Lett. 2024, 24, 7879−7885

■ ASSOCIATED CONTENT

Supporting Information

The Supporting Information is available free of charge at https://pubs.acs.org/doi/10.1021/acs.nanolett.4c01018.

(I) Experimental methods: tBLG sample preparation, Raman scattering measurements. (II–VII) Supplementary figures and analysis. Figure S1: atomic force microscopy (AFM) measurements and strain and doping analysis of suspended tBLG. Figure S2: optical setup of polarized Raman measurement. Figure S3: polarized Raman spectra of LB and ZATA mode. Figure S4: phonon dispersion and calculation of combinational probability. Figure S5: twist-angle-dependent Raman intensity of ZATA and LB. Figure S6: cyclic temperature-dependent Raman spectrum of LB and ZATA. Figures S7: incident power dependence of G, 2D, Si, LB, and ZATA (PDF)

■ AUTHOR INFORMATION

Corresponding Author

Lianming Tong − *Center for Nanochemistry, Beijing Science and Engineering Center for Nanocarbons, Beijing National Laboratory for Molecular Sciences, College of Chemistry and Molecular Engineering, Peking University, 100871 Beijing, China;* orcid.org/0000-0001-7771-4077; Email: tonglm@pku.edu.cn

Authors

Shuowen Yan − *Center for Nanochemistry, Beijing Science and Engineering Center for Nanocarbons, Beijing National Laboratory for Molecular Sciences, College of Chemistry and Molecular Engineering, Peking University, 100871 Beijing, China*

Jianqi Huang − *Shenyang National Laboratory for Materials Science, Institute of Metal Research, Chinese Academy of Sciences, Shenyang 110016, China; School of Material Science and Engineering, University of Science and Technology of China, Shenyang 110016, China; Liaoning Academy of Materials, Shenyang 110167, China*

He Hao − *Center for Nanochemistry, Beijing Science and Engineering Center for Nanocarbons, Beijing National Laboratory for Molecular Sciences, College of Chemistry and Molecular Engineering, Peking University, 100871 Beijing, China*

Ge Song − *Center for Nanochemistry, Beijing Science and Engineering Center for Nanocarbons, Beijing National Laboratory for Molecular Sciences, College of Chemistry and Molecular Engineering, Peking University, 100871 Beijing, China*

Yuechen Wang − *Center for Nanochemistry, Beijing Science and Engineering Center for Nanocarbons, Beijing National Laboratory for Molecular Sciences, College of Chemistry and Molecular Engineering and Academy for Advanced Interdisciplinary Studies, Peking University, 100871 Beijing, China; Beijing Graphene Institute, Beijing 100095, China*

Hailin Peng − *Center for Nanochemistry, Beijing Science and Engineering Center for Nanocarbons, Beijing National Laboratory for Molecular Sciences, College of Chemistry and Molecular Engineering and Academy for Advanced Interdisciplinary Studies, Peking University, 100871 Beijing, China; Beijing Graphene Institute, Beijing 100095, China;* orcid.org/0000-0003-1569-0238

Teng Yang − *Shenyang National Laboratory for Materials Science, Institute of Metal Research, Chinese Academy of Sciences, Shenyang 110016, China; School of Material Science and Engineering, University of Science and Technology of China, Shenyang 110016, China; Liaoning Academy of Materials, Shenyang 110167, China;* orcid.org/0000-0003-3773-7586

Jin Zhang − *Center for Nanochemistry, Beijing Science and Engineering Center for Nanocarbons, Beijing National Laboratory for Molecular Sciences, College of Chemistry and Molecular Engineering, Peking University, 100871 Beijing, China;* orcid.org/0000-0003-3731-8859

Complete contact information is available at: https://pubs.acs.org/10.1021/acs.nanolett.4c01018

Author Contributions

S.Y. prepared the specimens, performed all the Raman measurements, and proposed the possible scattering mechanism. J.H. provided phonon dispersion and calculations of combinational probability of low-frequency phonon pairs. L.T. and J.Z. supervised over all the experiments and data collection. All authors contributed to the discussion of data and writing of manuscript.

Notes

The authors declare no competing financial interest.

■ ACKNOWLEDGMENTS

This work was financially supported by the National Key R&D Program of China (2022YFA1203302, 2022YFA1203304 and 2018YFA0703502), the National Natural Science Foundation of China (Grant Nos. 52303291, 52021006, and 21974004), the Strategic Priority Research Program of CAS (XDB36030100), the Beijing National Laboratory for Molecular Sciences (BNLMS-CXTD-202001), and the Shenzhen Science and Technology Innovation Commission (KQTD20221101115627004).

■ REFERENCES

(1) Andrei, E. Y.; MacDonald, A. H. Graphene bilayers with a twist. *Nat. Mater.* **2020**, *19* (12), 1265–1275.

(2) Cao, Y.; Fatemi, V.; Demir, A.; Fang, S.; Tomarken, S. L.; Luo, J. Y.; Sanchez-Yamagishi, J. D.; Watanabe, K.; Taniguchi, T.; Kaxiras, E.; Ashoori, R. C.; Jarillo-Herrero, P. Correlated insulator behaviour at half-filling in magic-angle graphene superlattices. *Nature* **2018**, *556* (7699), 80–84.

(3) Park, J. M.; Cao, Y.; Xia, L.-Q.; Sun, S.; Watanabe, K.; Taniguchi, T.; Jarillo-Herrero, P. Robust superconductivity in magic-angle multilayer graphene family. *Nat. Mater.* **2022**, *21* (8), 877–883.

(4) Gadelha, A. C.; Ohlberg, D. A. A.; Rabelo, C.; Neto, E. G. S.; Vasconcelos, T. L.; Campos, J. L.; Lemos, J. S.; Ornelas, V.; Miranda, D.; Nadas, R.; Santana, F. C.; Watanabe, K.; Taniguchi, T.; van Troeye, B.; Lamparski, M.; Meunier, V.; Nguyen, V.-H.; Paszko, D.; Charlier, J.-C.; Campos, L. C.; Cançado, L. G.; Medeiros-Ribeiro, G.; Jorio, A. Localization of lattice dynamics in low-angle twisted bilayer graphene. *Nature* **2021**, *590* (7846), 405–409.

(5) Havener, R. W.; Liang, Y.; Brown, L.; Yang, L.; Park, J. Hove Singularities and Excitonic Effects in the Optical Conductivity of Twisted Bilayer Graphene. *Nano Lett.* **2014**, *14* (6), 3353–3357.

(6) Patel, H.; Havener, R. W.; Brown, L.; Liang, Y.; Yang, L.; Park, J.; Graham, M. W. Tunable Optical Excitations in Twisted Bilayer Graphene Form Strongly Bound Excitons. *Nano Lett.* **2015**, *15* (9), 5932–5937.

(7) Patel, H.; Huang, L.; Kim, C.-J.; Park, J.; Graham, M. W. Stacking angle-tunable photoluminescence from interlayer exciton states in twisted bilayer graphene. *Nat. Commun.* **2019**, *10* (1), 1445.
(8) Kim, C.-J.; Sánchez-Castillo, A.; Ziegler, Z.; Ogawa, Y.; Noguez, C.; Park, J. Chiral atomically thin films. *Nat. Nanotechnol.* **2016**, *11* (6), 520−524.
(9) Kim, K.; Coh, S.; Tan, L. Z.; Regan, W.; Yuk, J. M.; Chatterjee, E.; Crommie, M. F.; Cohen, M. L.; Louie, S. G.; Zettl, A. Raman Spectroscopy Study of Rotated Double-Layer Graphene: Misorientation-Angle Dependence of Electronic Structure. *Phys. Rev. Lett.* **2012**, *108* (24), 246103.
(10) Peng, H.; Schröter, N. B. M.; Yin, J.; Wang, H.; Chung, T.-F.; Yang, H.; Ekahana, S.; Liu, Z.; Jiang, J.; Yang, L.; Zhang, T.; Chen, C.; Ni, H.; Barinov, A.; Chen, Y. P.; Liu, Z.; Peng, H.; Chen, Y. Substrate Doping Effect and Unusually Large Angle van Hove Singularity Evolution in Twisted Bi- and Multilayer Graphene. *Adv. Mater.* **2017**, *29* (27), 1606741.
(11) Yin, J.; Wang, H.; Peng, H.; Tan, Z.; Liao, L.; Lin, L.; Sun, X.; Koh, A. L.; Chen, Y.; Peng, H.; Liu, Z. Selectively enhanced photocurrent generation in twisted bilayer graphene with van Hove singularity. *Nat. Commun.* **2016**, *7* (1), 10699.
(12) Saito, R.; Hung, N. T.; Yang, T.; Huang, J.; Liu, H.-L.; Gulo, D. P.; Han, S.; Tong, L. Deep-Ultraviolet and Helicity-Dependent Raman Spectroscopy for Carbon Nanotubes and 2D Materials. *Small* **2024**, 2308558.
(13) He, R.; Chung, T.-F.; Delaney, C.; Keiser, C.; Jauregui, L. A.; Shand, P. M.; Chancey, C. C.; Wang, Y.; Bao, J.; Chen, Y. P. Observation of Low Energy Raman Modes in Twisted Bilayer Graphene. *Nano Lett.* **2013**, *13* (8), 3594−3601.
(14) Wu, J.-B.; Zhang, X.; Ijäs, M.; Han, W.-P.; Qiao, X.-F.; Li, X.-L.; Jiang, D.-S.; Ferrari, A. C.; Tan, P.-H. Resonant Raman spectroscopy of twisted multilayer graphene. *Nat. Commun.* **2014**, *5* (1), 5309.
(15) Wu, J.-B.; Hu, Z.-X.; Zhang, X.; Han, W.-P.; Lu, Y.; Shi, W.; Qiao, X.-F.; Ijiäs, M.; Milana, S.; Ji, W.; Ferrari, A. C.; Tan, P.-H. Interface Coupling in Twisted Multilayer Graphene by Resonant Raman Spectroscopy of Layer Breathing Modes. *ACS Nano* **2015**, *9* (7), 7440−7449.
(16) Carozo, V.; Almeida, C. M.; Ferreira, E. H. M.; Cançado, L. G.; Achete, C. A.; Jorio, A. Raman Signature of Graphene Superlattices. *Nano Lett.* **2011**, *11* (11), 4527−4534.
(17) Eliel, G. S. N.; Moutinho, M. V. O.; Gadelha, A. C.; Righi, A.; Campos, L. C.; Ribeiro, H. B.; Chiu, P.-W.; Watanabe, K.; Taniguchi, T.; Puech, P.; Paillet, M.; Michel, T.; Venezuela, P.; Pimenta, M. A. Intralayer and interlayer electron−phonon interactions in twisted graphene heterostructures. *Nat. Commun.* **2018**, *9* (1), 1221.
(18) Campos-Delgado, J.; Cançado, L. G.; Achete, C. A.; Jorio, A.; Raskin, J.-P. Raman scattering study of the phonon dispersion in twisted bilayer graphene. *Nano Res.* **2013**, *6* (4), 269−274.
(19) Xu, B.; Hao, H.; Huang, J.; Zhao, Y.; Yang, T.; Zhang, J.; Tong, L. Twist-Induced New Phonon Scattering Pathways in Bilayer Graphene Probed by Helicity-Resolved Raman Spectroscopy. *J. Phys. Chem. C* **2022**, *126* (25), 10487−10493.
(20) Cocemasov, A. I.; Nika, D. L.; Balandin, A. A. Phonons in twisted bilayer graphene. *Phys. Rev. B* **2013**, *88* (3), No. 035428.
(21) Sun, L.; Wang, Z.; Wang, Y.; Zhao, L.; Li, Y.; Chen, B.; Huang, S.; Zhang, S.; Wang, W.; Pei, D.; Fang, H.; Zhong, S.; Liu, H.; Zhang, J.; Tong, L.; Chen, Y.; Li, Z.; Rümmeli, M. H.; Novoselov, K. S.; Peng, H.; Lin, L.; Liu, Z. Hetero-site nucleation for growing twisted bilayer graphene with a wide range of twist angles. *Nat. Commun.* **2021**, *12* (1), 2391.
(22) Pisana, S.; Lazzeri, M.; Casiraghi, C.; Novoselov, K. S.; Geim, A. K.; Ferrari, A. C.; Mauri, F. Breakdown of the adiabatic Born−Oppenheimer approximation in graphene. *Nat. Mater.* **2007**, *6* (3), 198−201.
(23) Zabel, J.; Nair, R. R.; Ott, A.; Georgiou, T.; Geim, A. K.; Novoselov, K. S.; Casiraghi, C. Raman Spectroscopy of Graphene and Bilayer under Biaxial Strain: Bubbles and Balloons. *Nano Lett.* **2012**, *12* (2), 617−621.
(24) Lee, J. E.; Ahn, G.; Shim, J.; Lee, Y. S.; Ryu, S. Optical separation of mechanical strain from charge doping in graphene. *Nat. Commun.* **2012**, *3* (1), 1024.
(25) Chandrasekhar, M.; Cardona, M.; Kane, E. O. Intraband Raman scattering by free carriers in heavily doped n-Si. *Phys. Rev. B* **1977**, *16* (8), 3579−3595.
(26) Tan, P. H.; Han, W. P.; Zhao, W. J.; Wu, Z. H.; Chang, K.; Wang, H.; Wang, Y. F.; Bonini, N.; Marzari, N.; Pugno, N.; Savini, G.; Lombardo, A.; Ferrari, A. C. The shear mode of multilayer graphene. *Nat. Mater.* **2012**, *11* (4), 294−300.
(27) Yoon, D.; Moon, H.; Son, Y.-W.; Choi, J. S.; Park, B. H.; Cha, Y. H.; Kim, Y. D.; Cheong, H. Interference effect on Raman spectrum of graphene on SiO_2/Si. *Phys. Rev. B* **2009**, *80* (12), 125422.
(28) Coh, S.; Tan, L. Z.; Louie, S. G.; Cohen, M. L. Theory of the Raman spectrum of rotated double-layer graphene. *Phys. Rev. B* **2013**, *88* (16), 165431.
(29) Zobeiri, H.; Xu, S.; Yue, Y.; Zhang, Q.; Xie, Y.; Wang, X. Effect of temperature on Raman intensity of nm-thick WS2: combined effects of resonance Raman, optical properties, and interface optical interference. *Nanoscale* **2020**, *12* (10), 6064−6078.
(30) Lai, J.-M.; Sun, Y.-J.; Tan, Q.-H.; Tan, P.-H.; Zhang, J. Laser Cooling of a Lattice Vibration in van der Waals Semiconductor. *Nano Lett.* **2022**, *22* (17), 7129−7135.
(31) Varshni, Y. P. Temperature dependence of the energy gap in semiconductors. *Physica* **1967**, *34* (1), 149−154.
(32) Ho, C. H.; Wu, C. S.; Huang, Y. S.; Liao, P. C.; Tiong, K. K. Temperature dependence of energies and broadening parameters of the band-edge excitons of single crystals. *J. Phys. Condens. Mater.* **1998**, *10* (41), 9317.
(33) Goldstein, T.; Chen, S.-Y.; Tong, J.; Xiao, D.; Ramasubramaniam, A.; Yan, J. Raman scattering and anomalous Stokes−anti-Stokes ratio in MoTe2 atomic layers. *Sci. Rep.* **2016**, *6* (1), 28024.
(34) Zhang, J.; Zhang, Q.; Wang, X.; Kwek, L. C.; Xiong, Q. Resolved-sideband Raman cooling of an optical phonon in semiconductor materials. *Nat. Photonics* **2016**, *10* (9), 600−605.

https://doi.org/10.1021/acs.nanolett.4c01018
Nano Lett. 2024, 24, 7879−7885